ELSEVIER

Journal of Structural Geology 29 (2007) 646–663

JOURNAL OF STRUCTURAL GEOLOGY

www.elsevier.com/locate/jsg

Fault superimposition and linkage resulting from stress changes during rifting: Examples from 3D seismic data, Phitsanulok Basin, Thailand

C.K. Morley*, S. Gabdi, K. Seusutthiya

PTTEP, 555 Vibhavadi-Rangsit Road, Chatuchak, Bangkok 10900, Thailand

Received 15 May 2006; received in revised form 22 October 2006; accepted 18 November 2006
Available online 18 January 2007

Abstract

The Phitsanulok basin, Thailand provides examples of changing fault displacement patterns with time associated with faults of different orientations. In the Northern Phitsanulok basin three main stress states have been identified associated with Late Oligocene–Recent fault development: (1) Late Oligocene–Late Miocene approximately E–W extension (N–S Shmax), 'main rift' stage, (2) Late Miocene–Pliocene transtension to tranpression (?) (E–W to NE–SW Shmax), 'late rift' stage, and (3) Pliocene–Recent very minor faulting, E–W extension, N–S Shmax, 'post-rift' stage. Syn-rift faults tend to strike N–S, but also follow NE–SW and NW–SE trends and are basement involved. The Late Miocene deformation produced a distinctly different type of fault population from the main rift fault set, characterized by numerous, small displacement (tens of metres), faults striking predominantly NE–SW. Most of these faults are convergent, conjugate sets aligned in discrete zones and nucleated within the sedimentary basin. Reactivation of main rift faults trends during the late rift stage favoured strike directions between 350° and 50°. The displacement characteristics of three large faults within the basin show variations depending upon fault orientation. The low-angle (23°-30° dip), Western Boundary Fault (~7 km throw) displays little discernible difference in the distribution of displacement on fault zone during the different stress states other than increases and decreases in displacement amount. Smaller faults exhibit a more selective reactivation history than the Western Boundary fault and are more informative about fault response to a varying stress field. Activation of the (oblique) NE–SW striking NTM-1 initially produced a fault divided into three segments, splaying into N–S trends. Stress reorientation during the late rift stage finally linked NE–SW striking segments. The partial linkage of the fault zone at the time of oil migration resulted in the southwestern part of the NTM-1 fault sealing hydrocarbon bearing reservoirs, whilst late linkage areas along the northeastern part failed to seal hydrocarbons. The N–S striking PTO-1 Fault shows early isolated fault segments, linkage during syn-rift motion, then a more patchy distribution of displacement late in the fault history, perhaps due to non-optimal orientation of the fault to the regional stress field, when compared with the NTM-1 Fault. The fault characteristics described indicate that where strong pre-existing fabrics are present, and varying stress regimes have occurred, fault population characteristics and evolution of fault displacement can depart considerably from extensional fault populations associated with a single phase of extension.

Keywords: Extension; Displacement; Fabric inheritance; Thailand

1. Introduction

A number of studies have documented the fundamental characteristics of fault displacement–length relationships and fault evolution, propagation and linkage (e.g. Barnett et al., 1987; Walsh and Watterson, 1988, 1992; Peacock and Sanderson, 1991; Cartwright et al., 1995; Huggins et al., 1995). One of the fundamental resulting conclusions is that fault displacement and fault length tend to show a linear, power law relationship on log–log graphs. Consequently as a fault increases displacement so its length should also increase, particularly when a fault develops by lateral propagation from the centre (isolated fault model, Fig. 1a). Fault linkage models reflect the common, if not ubiquitous, situation that a rock volume contains numerous faults and fractures, as

* Corresponding author. Tel.: +66 2 235 2464.
E-mail address: chrissmorley@gmail.com (C.K. Morley).

0191-8141/$ - see front matter © 2007 Elsevier Ltd. All rights reserved.
doi:10.1016/j.jsg.2006.11.005

faults increase in length they interact, and some faults and fractures meet and join (Fig. 1). Hence development of fault length and displacement is partially independent (e.g. Barnett et al., 1987; Walsh and Watterson, 1987; Schlische, 1991; Cowie and Schloz, 1992; Davison, 1994; Cartwright et al., 1995; Schlische and Anders, 1996; Morley, 1999a). For some faults linkage occurs early and much of their displacement history is one of building displacement without lateral propagation (Fig. 1c). For other faults much of their displacement history is characterised by displacement on independent segments and final linkage of the fault zone occurs late in the fault history (Fig. 1b).

Another aspect of fault evolution in rift basins is the tendency for deformation to be concentrated on progressively larger faults with time, and for small faults to become inactive (e.g. Cowie, 1998; Gupta et al., 1998). This tendency has been demonstrated for simple rifts, but what happens in situations complicated by strong pre-existing fabrics and variable regional stress orientations is not well described.

The development of normal fault populations under relatively simple single extensional episodes, and constant regional stress as discussed above is now well documented. Development under more complex conditions of varying principal stress orientation and the extensive presence of weak fabrics oriented oblique to the extension direction has not been so extensively investigated. Given the long history of activity in many basins, such development may be more the rule than the simplest models for fault linkage and evolution. This study investigates the effects of oblique fabrics and changing regional stress on fault displacement, length and orientation using 3D seismic data from the Phitsanulok basin of central Thailand (Fig. 2). This paper builds on previous work on the rift basins of Thailand that investigated the influence of pre-rift fabrics on syn-rift fault geometry, and how changing stress orientations resulted in late faults inheriting oblique fabrics from the syn-rift faults (Kornsawan and Morley, 2002; Morley et al., 2004). Where fabric inheritance is very strong the characteristics of fault populations can depart from the linear length-displacement plots of typical fault populations (Morley et al., 2004).

Appreciation of fault linkage patterns also has applications for the oil industry. The various modes of fault development give rise to different timing of trap closure, and different timing as to when a fault may become a significant barrier to hydrocarbon migration. Linkage of major faults can also impact the timing of when and how faults exert an influence on sediment pathways, and whether basin development is characterised by merging of small, isolated basins with time, or whether one large basin has been prevalent (e.g. Young et al., 2001; Talbot et al., 2005).

2. Geology of the Phitsanulok Basin

The Phitsanulok Basin is the largest of a string of N–S trending late Cenozoic rift basins that run through central Thailand. The basin is about 140 km long and 40 km wide. It contains the largest onshore oil and gas field in Thailand; the

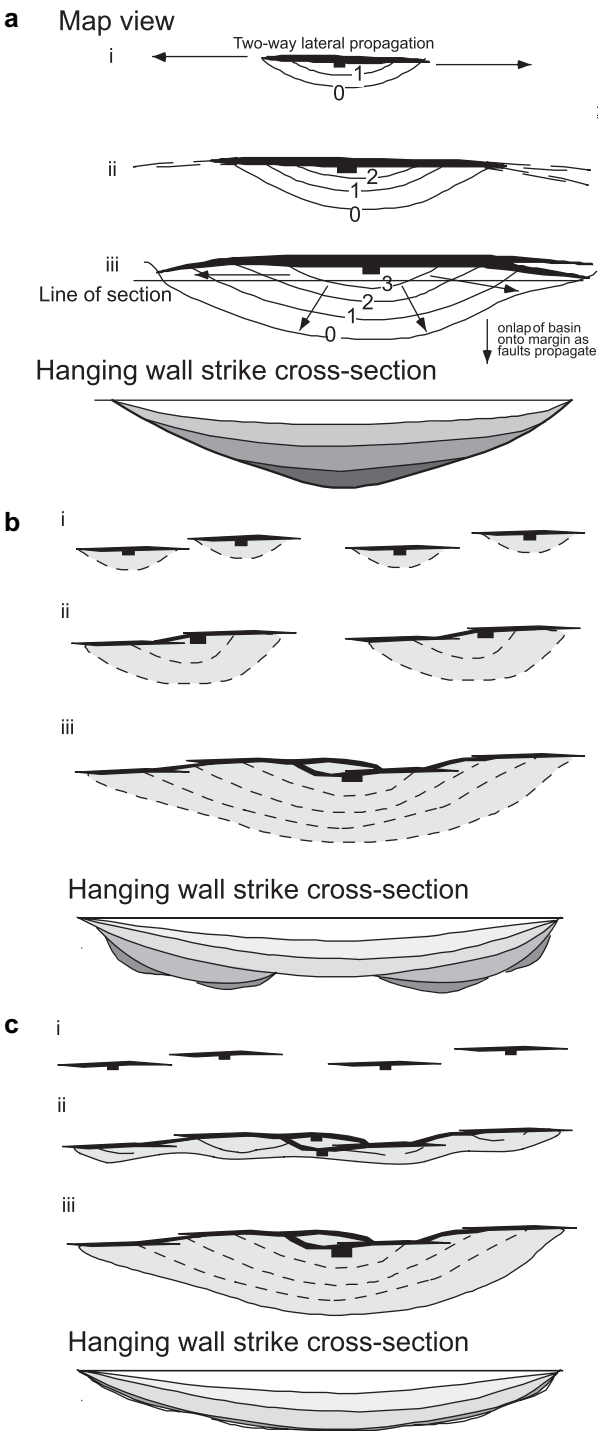

Fig. 1. Schematic illustration of three basic ways in which fault systems may develop and how displacement (and syn-kinematic sedimentary basins) may progressively build on the faults. (a) Isolated radial propagation: an isolated fault grows by progressively increasing in length by lateral propagation and increasing in displacement. Commonly the location of maximum displacement will remain fixed (e.g. Barnett et al., 1987). (b, c) Increase in fault length by radial propagation and linkage with other faults. In (b) fault linkage is gradual with respect to the building of fault displacement. Hence the displacement profile of the fault is irregular, reflecting displacements on the earlier isolated faults (e.g. Schlische and Anders, 1996). In (c) the other extreme is illustrated where the fault linkage occurred very early in the propagation history so the fault displacement profile is smooth and dominated by the displacement on the fault post-linkage (e.g. Morley, 1999a). Modified from Morley and Wonganan (2000).

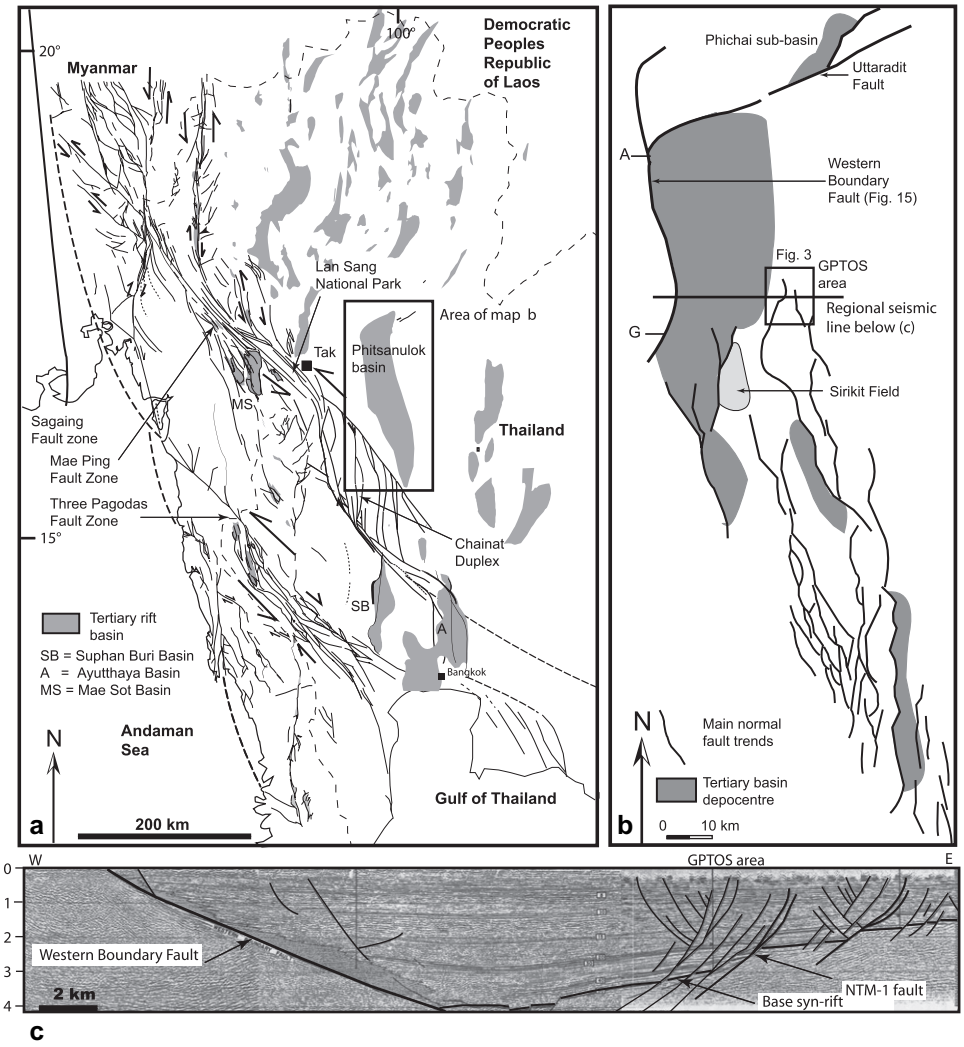

Fig. 2. Location map for the Phitsanulok Basin in Thailand.

Sirkit Field (Fig. 2). Smaller oil fields are found to the northeast of the field in the Greater Pratu Tao south area (GPTOS; Fig. 1). It is the GPTOS area that is the focus of this study. The northern half of the basin is dominated by two large faults, the N–S striking Western Boundary Fault, which controls subsidence in the main Phitsanulok Basin, and the ENE–WSW striking Uttardit Fault which controls subsidence in the northern-most Phichai sub-basin (Fig. 2). Papers which summarize the stratigraphy of the basin include Knox and Wakefield (1983), Flint et al. (1988), and Bal et al. (1992). Deposition occurred in a continental setting from the Late Oligocene–Recent (Fig. 4). Stratigraphic nomenclature is based on lithostratigraphy, hence as specific depositional environments occur at different times in different parts of the basin the formation tops and bottoms are laterally variable and time transgressive. For the GPTOS area the following formations are used (Fig. 4): (1) Late Oligocene, Nong Bua Formation, predominantly alluvial plain deposits, (2) Early Miocene, Lan Krabu Formation, lacustrine-deltaic deposits, (3) Early Miocene, Chum Saeng Formation, open lake, (4) Middle Miocene, Pratu Tao Formation, alluvial plain deposits, and (5) Late Miocene–Pliocene, Yom and Ping Formations, alluvial plain to alluvial fan deposits.

The papers by Knox and Wakefield (1983), Flint et al. (1988), and Bal et al. (1992) propose a strong component of strike-slip deformation has affected the basin. The interpretation was based on regional tectonic models prevalent at the time and 2D seismic data. The current interpretation of the basin based on 2D and 3D seismic data, and more detailed interpretation of the surrounding geology indicates the basin evolved primarily under approximately E–W extension, but did experience episodes of inversion during the Miocene that could have occurred under conditions ranging from transtension to compression (e.g. Morley et al., 2004). One of these episodes (Late Miocene) affected the northern part of the basin and is discussed in detail in this paper.

3. Basin evolution

The overall structural evolution of the northern half of the Phitsanulok basin from the Late Oligocene to Middle

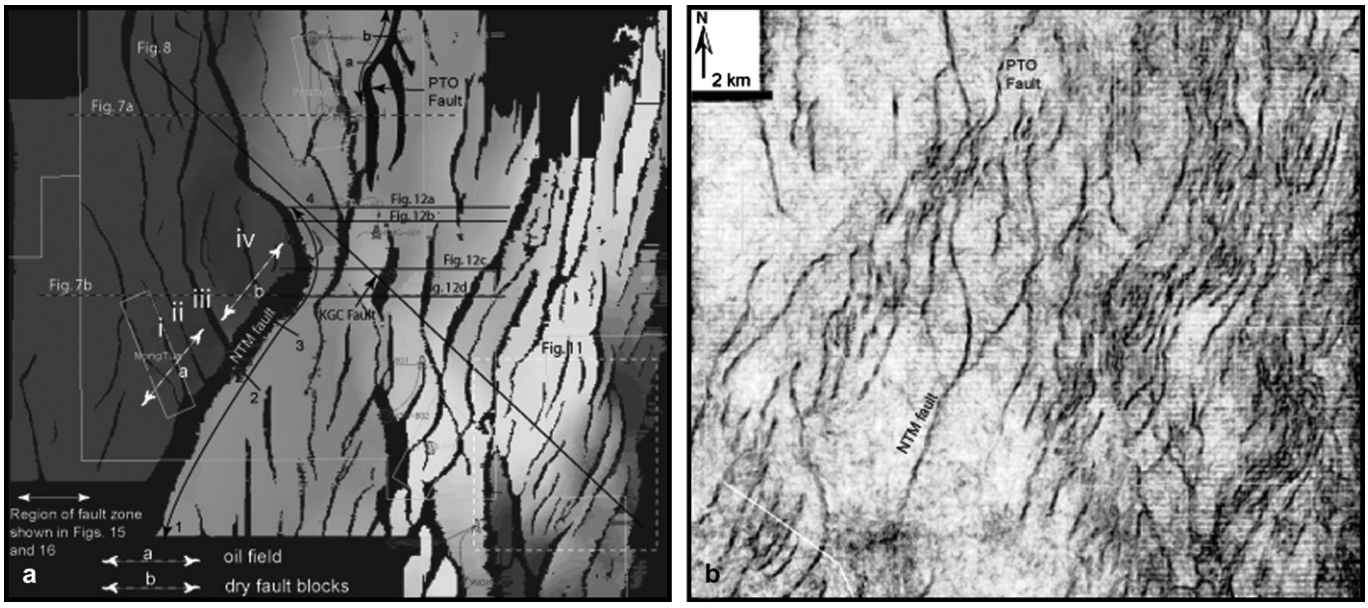

Fig. 3. Time–structure map of the top Chum Saeng Formation (early Miocene). Coherency map time slice at 600 ms (approximate depth of Yom and Ping Formations) illustrating the shallow fault pattern. See Fig. 2 for map location.

Miocene appears to have been dominated by extension. Faults predominantly trend N–S, but other important orientations are NW–SE and NE–SW to ENE–WSW (Fig. 3a). These orientations coincide with known pre-existing trends in basement, for example the ENE–WSW trending Uttaradit Fault (Fig. 2) follows the strike of the Palaeozoic Nan-Uttaradit Suture, NW–SE and NE–SW trends coincide in both orientation and scale with thrust and fold trends of Late Cretaceous–Early Cenozoic age immediately west of the Phitsanulok basin (Fig. 2). In places seismic reflection data shows basement reflections have the geometry of folds associated with imbricate thrusts that have later been followed by normal faults (Fig. 5d).

The overall pattern of structural activity in the northern Phitsanulok basin can be seen in a burial history plot for the main depocentre (Fig. 4) The Oligocene–Early Miocene subsidence is relatively slow, then increased during Lan Krabu–Chum Saeng Formation times. The most rapid subsidence occurred in the latest Early Miocene–Middle Miocene, during deposition of the Pratu Tao Formation. Subsidence from the Late Miocene–Recent has slowed considerably during Yom Formation and Ping Formation times.

In the Late Miocene there is clear evidence for a change in stresses both regionally (e.g. Morley et al., 2000, 2001; Morley, 2007) and affecting different areas in the Phitsanulok

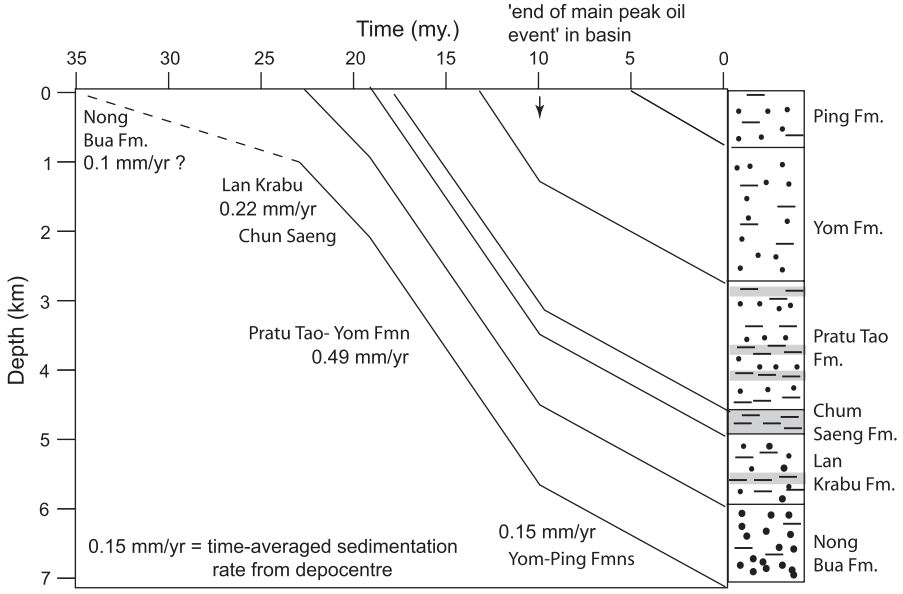

Fig. 4. Burial history plot for the main Phitsanulok basin depocentre based on seismic across the deepest part of the basin.

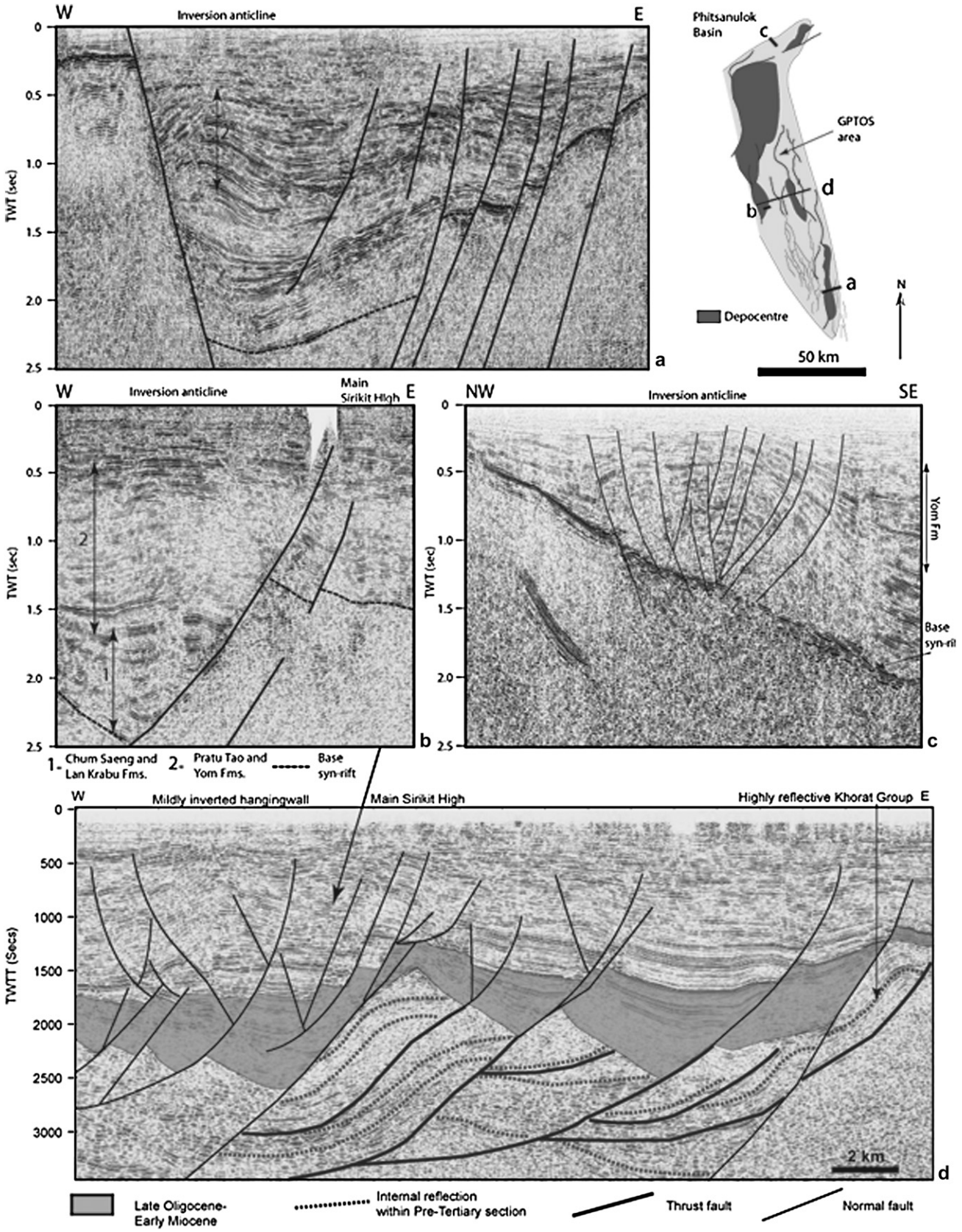

Fig. 5. 2D seismic lines illustrating Late Miocene inversion in different parts of the Phitsanulok basin. (a) Inversion of half graben bounding fault, Nong Bua Basin, southern Phitsanulok basin. (b) Inversion of hangingwall of fault bounding the Sirikit Field tilted fault block, central Phitsanulok basin. (c) Inversion near flexural margin of half graben, northern Phitsanulok basin (Pichit sub-basin). Note there is very little detectable offset of the strong base syn-rift reflection, but numerous faults are present within the syn-rift section. Inversion appears to be about 100% resulting in the absence of offset at the base syn-rift horizon whilst the overlying section has a strongly domed appearance. (d) Regional seismic line through the Sirikit Field illustrating the presence of an imbricate thrust geometry in pre-rift basement. Several of these thrusts appear to have been reactivated by normal faults; there is a strong west-dipping bias to the normal fault orientations coincident with the predominant dip of thrusts and bedding in the Mesozoic section. The western part of the line displays a gentle inversion anticline that is better developed along strike (line b).

basin. This change in stress caused minor inversion along the N–S striking bounding fault of the Nong Bua sub-basin in the southern part of the Phitsanulok basin (Fig. 5a). In the northern part of the basin the Uttaradit Fault developed an inversion anticline during the Late Miocene at a NE–SW trending jog, indicating fault motion had changed from oblique (sinistral) extension to a right-lateral component of motion indicating an approximately E–W Shmax direction (Morley et al., 2004). Other inversion features occur nearby (Fig. 5b). Late inversion is also seen along parts of the fault zone bounding the western side of Sirikit Field (Fig. 5c,d). However the most widespread effect of the stress change is seen in minor faults on the eastern side of the basin, and can only be demonstrated due to the acquisition of 3D seismic data over the area. During Yom Formation times a series of minor conjugate fault systems developed (Figs. 3b, 6 and 7). Since most of the basin subsidence was finished during Yom Formation times (Fig. 5) the Late Oligocene–Early Late Miocene fault pattern will be referred to as main rift, whilst the Yom Formation fault pattern is called late rift. The late rift faults generally have normal

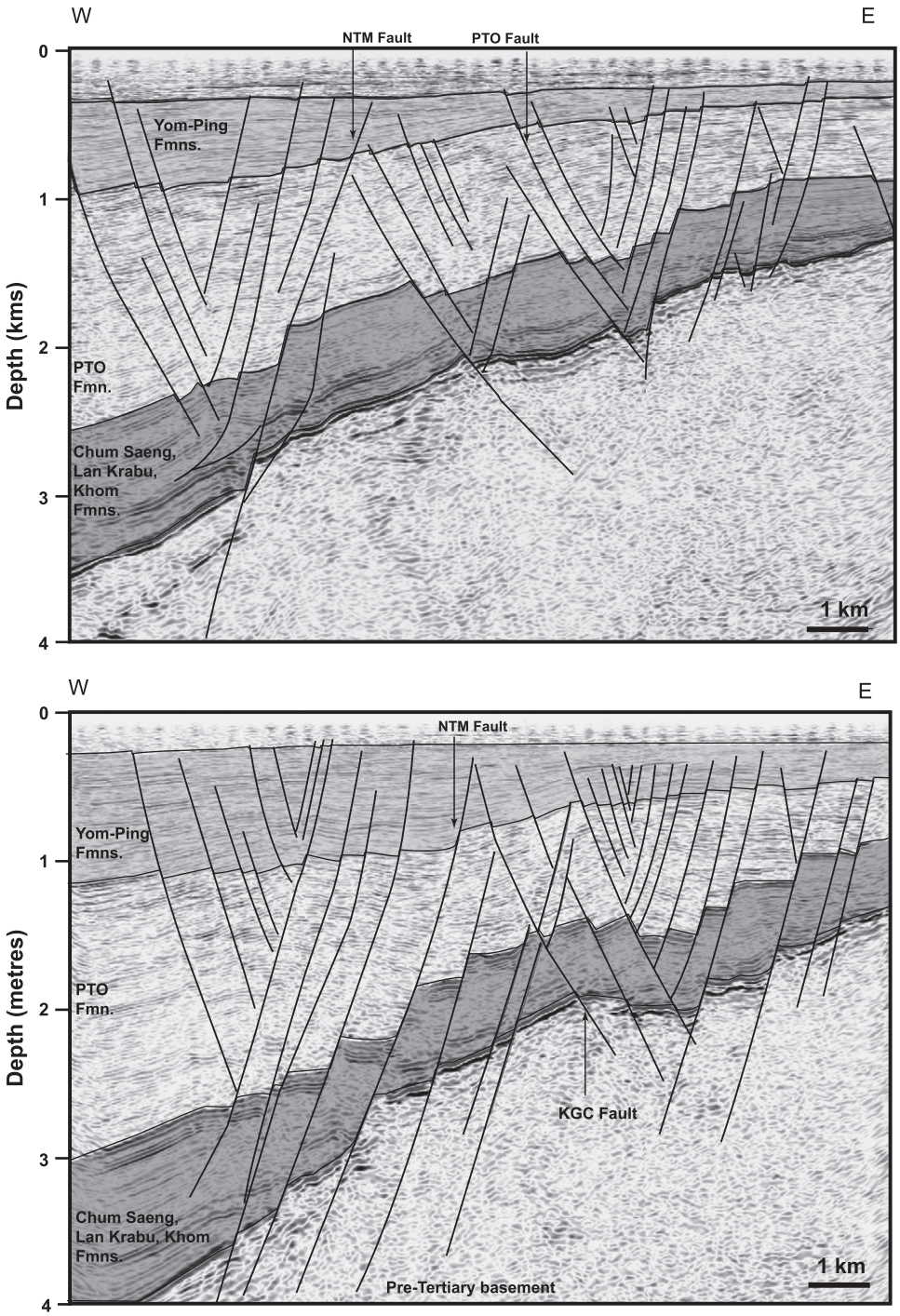

Fig. 6. 3D inline sections illustrating the typical geometry of the main rift and late rift faults. See Fig. 3 for location.

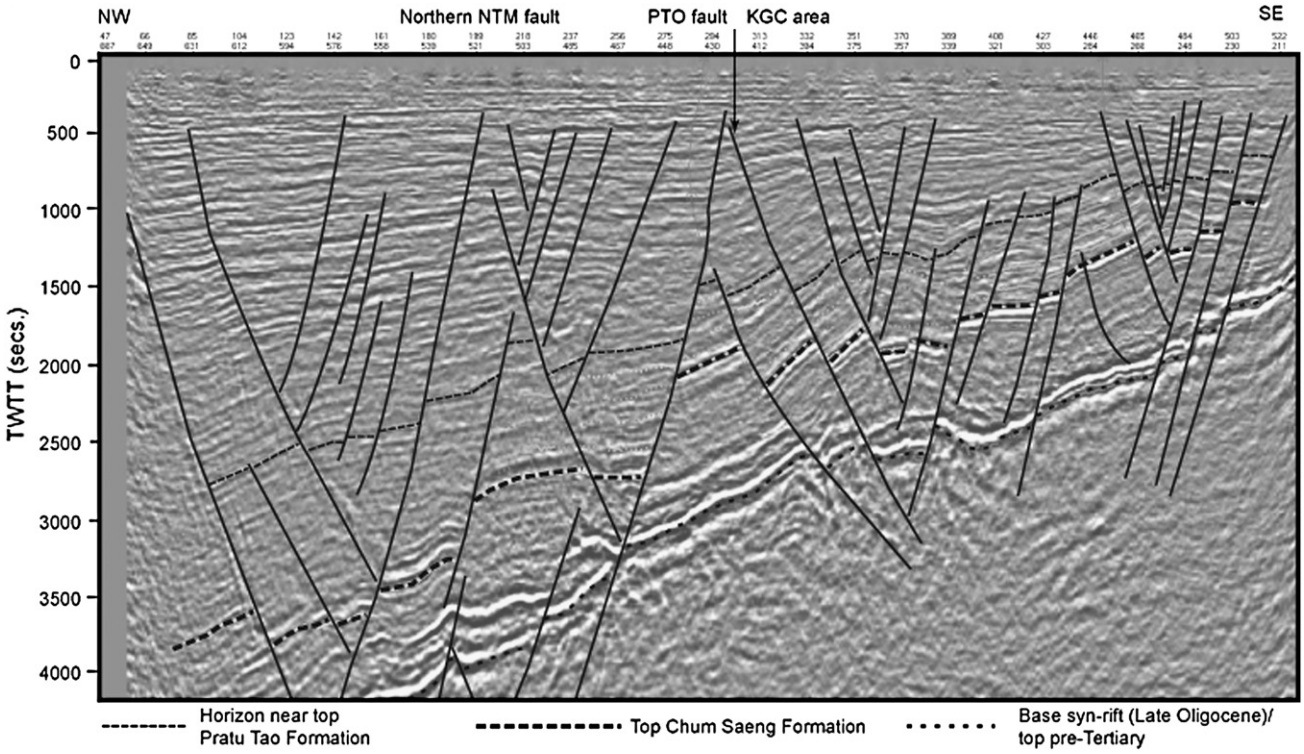

Fig. 7. 3D NW–SE trending random line illustrating the typical convergent conjugate geometry of late rift faults and associated broad antiformal geometry of seismic reflections. See Fig. 3 for location.

fault senses of displacement in the order of tens of metres, they are not very large, but they are numerous (Figs. 6, 7 and 9). The late rift faults tend to form conjugate sets that converge at depth, they define discrete zones, and have created broad antiforms with gently dipping limbs (up to 5° dip) (Figs. 6 and 7). The antiformal geometry may have two possible origins, either they are: (1) just the result of small rotations of bedding associated with conjugate normal fault displacement, or (2) in addition to that mechanism they also developed due to a compressional component of deformation associated with strain partitioning in a transtensional setting (De Paola et al., 2005). On 2D seismic data the conclusion is likely to be the anticlines originated due to (1) above because faults may be miscorrelated, and deeper and shallower faults mistakenly linked. However, 3D seismic data shows the Yom Formation minor fault pattern is actually considerably different from the underlying fault pattern. The main rift NW–SE trends tend to be ignored by the late rift faults, and are in places crossed by overlying NE–SW trending faults; whilst NE–SW trends and N–S trends, where present, are reactivated. Late rift faults that do not reactive older faults are mostly oriented NE–SW (Figs. 3, 9 and 10).

Given the change in fault orientation, presence of inversion features elsewhere in the basin (Fig. 4), and the association of anticlines with conjugate normal faults it is inferred that the late rift faults developed during a regional change in stress regime from extension to one that promoted transtensional to transpressional deformation (that locally varied in character but resulted in widespread inversion). The orientation of the anticlines, and the inversion anticline at the NE–SW restraining bend along the Uttaradit fault, suggests the NE–SW fault trends have a dextral component of strike-slip motion, which in turn indicates the Shmax direction was oriented somewhere between NE–SW and ENE–WSW (Fig. 8). This is consistent with inversion anticlines found along N–S trending faults elsewhere in the basin (Fig. 5a,c,d). The anticline in Fig. 5c helps illustrate the problem with interpreting the origin of the anticlines in the GPTOS area. The steeper anticline limbs (compared with the GPTOS area), uplift and erosion at the crest and absence of offset at the basement level indicates an inversion anticline. Yet rotation and expansion of section into many of the faults indicates an extensional component to these 'inverted' faults. Similar styles of faults and anticlines that are clearly associated with less ambiguous inversion structures are seen in the Anza Graben of Kenya (Morley, 1999b). The actual evolution of this kind of anticline is not well understood; for example do the faults evolve by alternating pulses of extension and compression or strike-slip motion or is there strain partitioning between extensional and strike-slip faults (e.g. De Paola et al., 2005)? Such basic questions are difficult to address because on 2D seismic data it is very difficult to reliably carry horizons across all the faults in the structure. The authors are unaware of any physical model that has attempted to reproduce these particular kinds of anticlines and document their origin. We interpret these anticlines in the GPTOS area as an early-stage equivalent of these inversion anticlines given their timing coincident with inversion features elsewhere in the basin and the change in fault patterns.

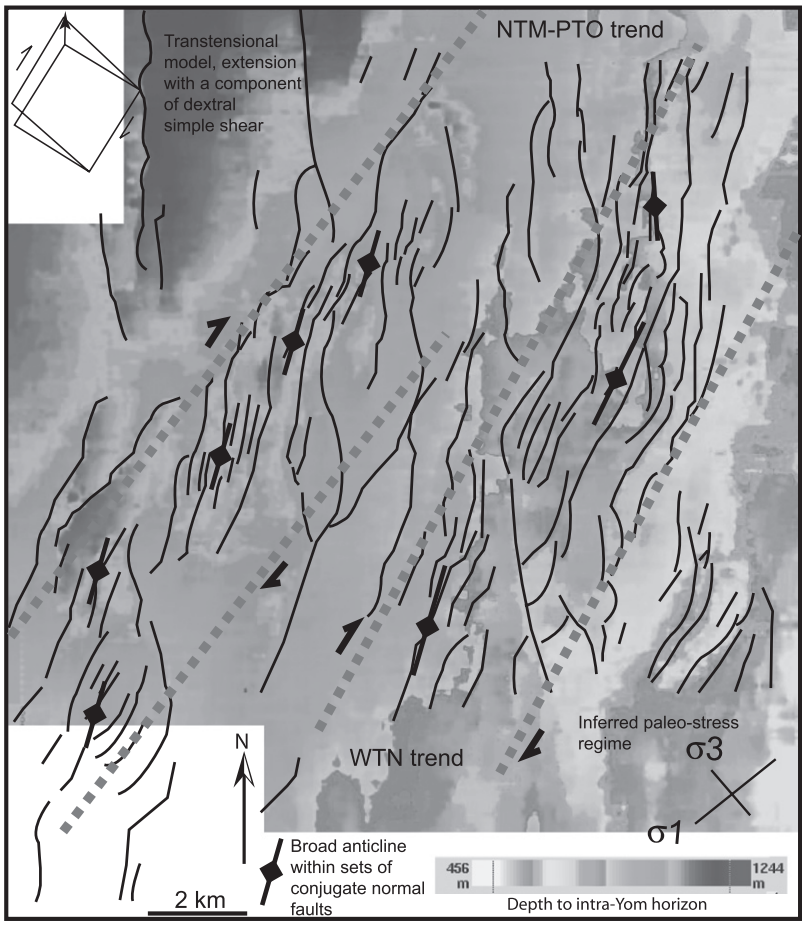

Fig. 8. Time–structure map of an intra-Yom Formation horizon illustrating the strong NE–SW bias to fault trends in the shallow subsurface. The basin is deepest in the northwestern area and overall shallows to the SE. The orientation of the broad antiformal faults, and the predominantly extensional nature of the faults suggests the late deformation was transtensional. Shmax during this time was probably oriented E–W to NE–SW. For inversion structures in other parts of the basin a more E–W orientation seems appropriate. In the GPTOS area to activate NE–SW to N–S trends suggests that at least in GPTOS the Shmax direction was NE–SW. Two main corridors of conjugate fault sets can be identified, which are labelled the NTM-PTO and WTN trends.

However, at this stage in our understanding the explanation has many ambiguities and a simple extensional origin between conjugate normal fault sets for the anticlines cannot be discounted. If the anticlines are extensional in origin then a change from E–W to NW–SE extension is inferred for the late rift stage.

The modern stress state determined regionally by earthquake focal mechanisms, and locally by borehole breakout data from wells show that today the maximum horizontal stress direction is N–S (Morley, 2007). Hence the Ping Formation history points to the stress orientations today being similar to those for the Late Oligocene–Middle Miocene. However the stress magnitudes are different, most faults are inactive today, and the active faults display only minor displacements. Essentially the latest deposition (upper few hundred metres) within the basin can be viewed as post-rift.

4. Fault geometries

The upwards loss of displacement on basement-involved faults indicates the main rift faults nucleated from basement and propagated up into the rift basin sediments (Figs. 11 and 12). Yet the late rift faults appear to have mostly nucleated within the sedimentary section and propagated downwards, since many demonstrably late faults decrease in displacement downwards as well as upwards (Figs. 7 and 12). Many faults do not reach basement and die out without the base syn-rift reflection being offset (Fig. 7). In the clearest cases the NE–SW striking late rift faults die out just above the base syn-rift reflection, and reflections from the syn-rift section are more highly rotated than the base syn-rift reflection. Adjacent N–S trending main rift faults are present, but die out at about levels of the Chum Saeng Formation or Pratu Tao Formation, and do not link with the late rift faults (Figs. 10–12). In other examples the base syn-rift reflection is offset by considerably smaller amounts than the syn-rift section. Fig. 11 shows one example of a fault that formed by lateral linkage of a main rift and late rift fault. The northern part of the fault is a main rift fault that shows greatest offset in basement and the fault dies out upwards, the southern part of the fault is a late rift fault that crosses a much younger part of the section and dies out downwards.

In many instances the relationship between main rift and late rift faults is indistinct, the faults show similar strikes,

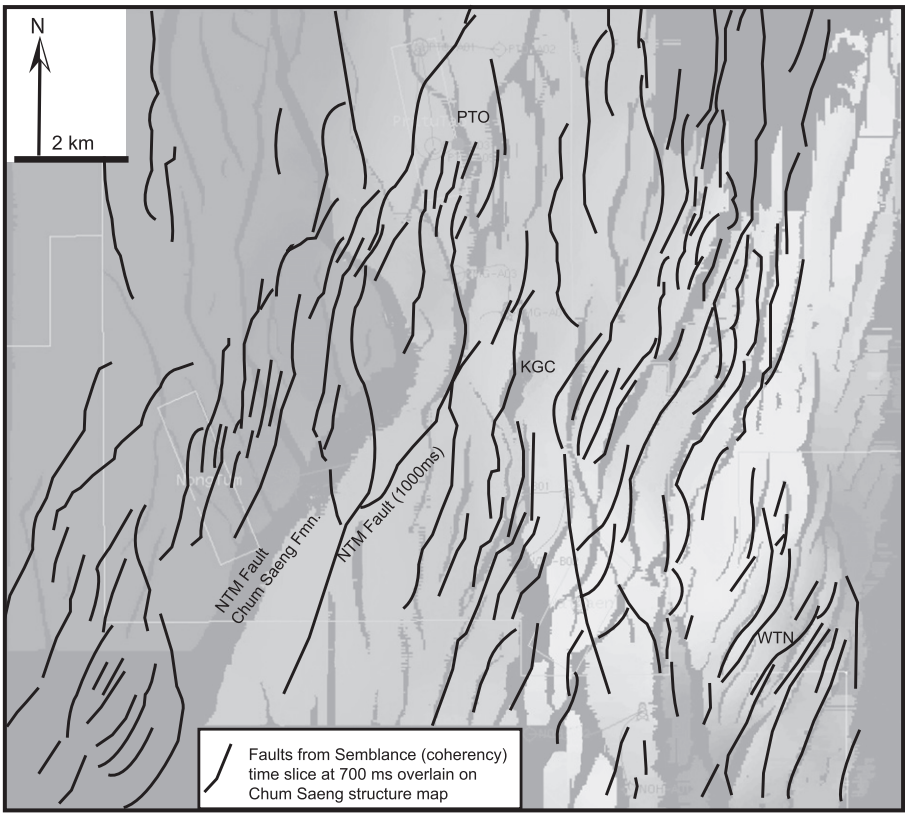

Fig. 9. Overlay of fault patterns at the Chum Saeng level (map with structure contours) and from a 700 ms time-slice (approximately Yom Formation level, black faults). This map illustrates where fault trends at the two mapped levels are similar and where they differ. In particular north of the NTM fault the shallow fault pattern is predominantly NE–SW whilst at the Chum Saeng Formation level the dominant trend is NW–SE to N–S.

and dips, and have linked without any major differences being apparent. Particularly in the deeper parts of the section where late rift convergent conjugate faults meet the fault pattern becomes difficult to interpret from seismic data (Figs. 6 and 7): not only are there numerous cross-cutting conjugate fault offsets to resolve, but the main rift faults with a different strike orientation are also offset by the later conjugate faults. The evolution of two of the large fault systems that have linked

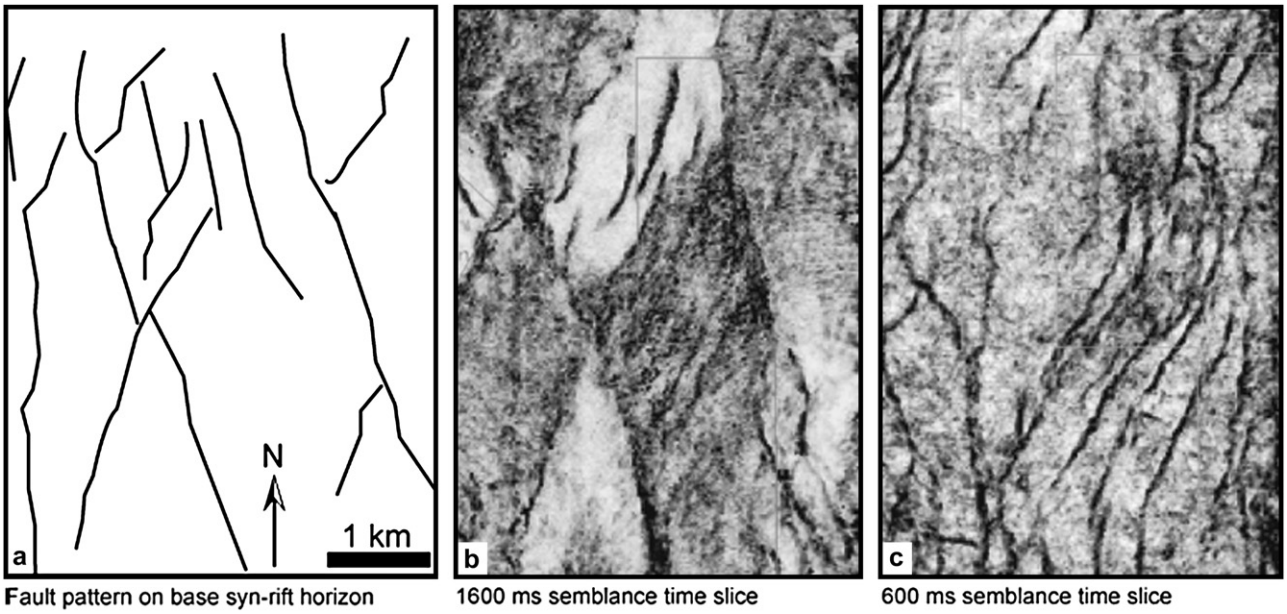

Fig. 10. Detail of the WTN area where at the base syn-rift the fault orientations shows a mix between NW–SE, N–S and NE–SW. Passing higher through the section the NW–SE trend becomes much less important and the NE–SW trends become more prominent. See Fig. 3 for location.

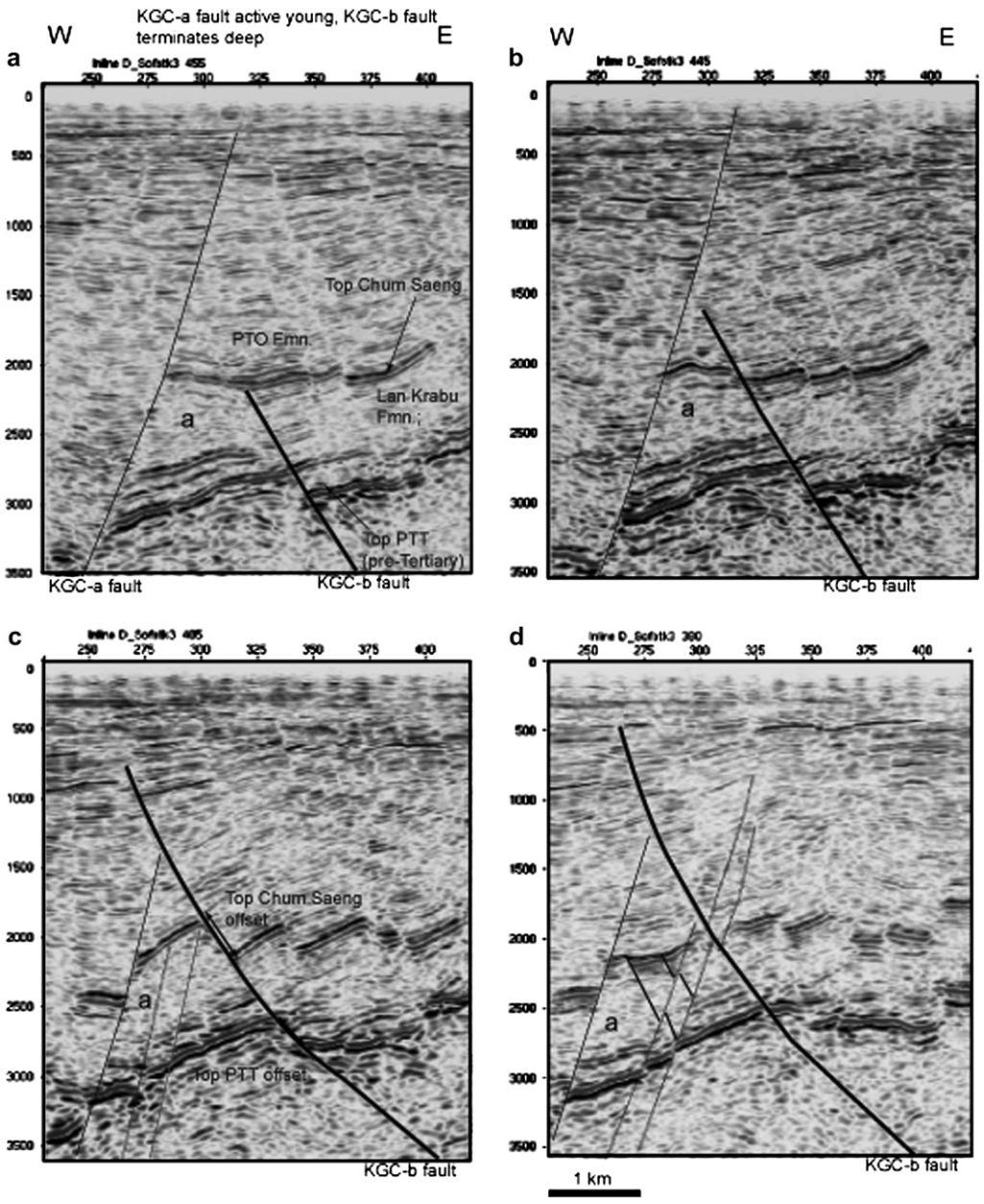

Fig. 11. Seismic lines across the KGCb fault show the fault having main rift fault characteristics in the north (a, b) and pass to a more late rift fault style in the south (c, d).

and display both main rift and late rift displacements is discussed below.

The fault population of the GPTOS area is composed of the following fault types (Fig. 12): (1) main rift faults that propagated up from the pre-Cenozoic section and ceased development during the Early or Middle Miocene. (2) main rift faults that continued to reactivate during the late rift stage. (3) late rift faults nucleated within the sedimentary basin section that have linked either laterally or downwards with segments of main rift faults; and (4) late rift faults that are not linked with main rift faults.

For many faults the displacements are too small to resolve the detailed evolution of fault displacement from horizon offsets on 3D data. For some larger faults the detailed evolution can be resolved. Three such faults are discussed below: the NTM-1 fault which is the largest oblique (NE–SW) trending fault in the GPTOS area, the PTO fault which is a large N–S trending fault (see Fig. 3 for locations), and the Western Boundary Fault (see Fig. 2 for location).

5. NTM-1 Fault

The NTM-1 fault trends NE–SW along much of its length and curves northwards into a N–S direction (Fig. 3). The fault forms the southern boundary to several fault-bounded hydrocarbon accumulations, and provides critical closure at the southern end of the blocks. At several places along the fault there are N–S trending splays (Fig. 13, faults i–iv). When

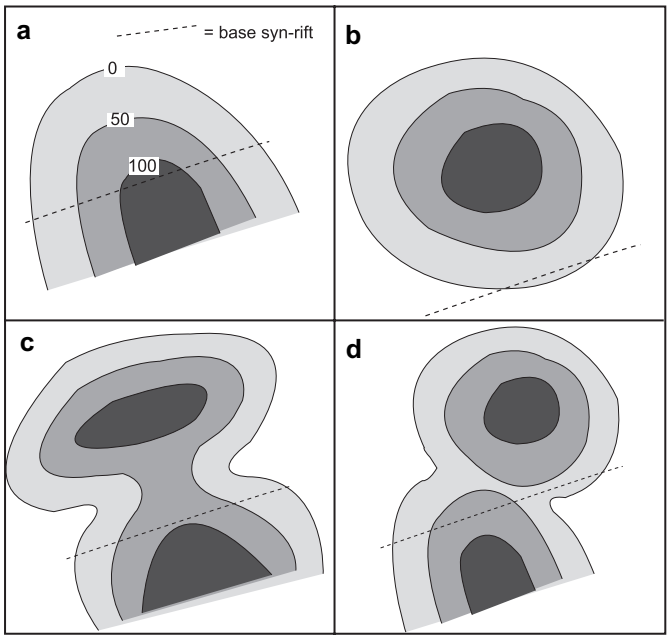

Fig. 12. Schematic illustration of the basic types of fault displacement contour pattern seen in the GPTOS area.

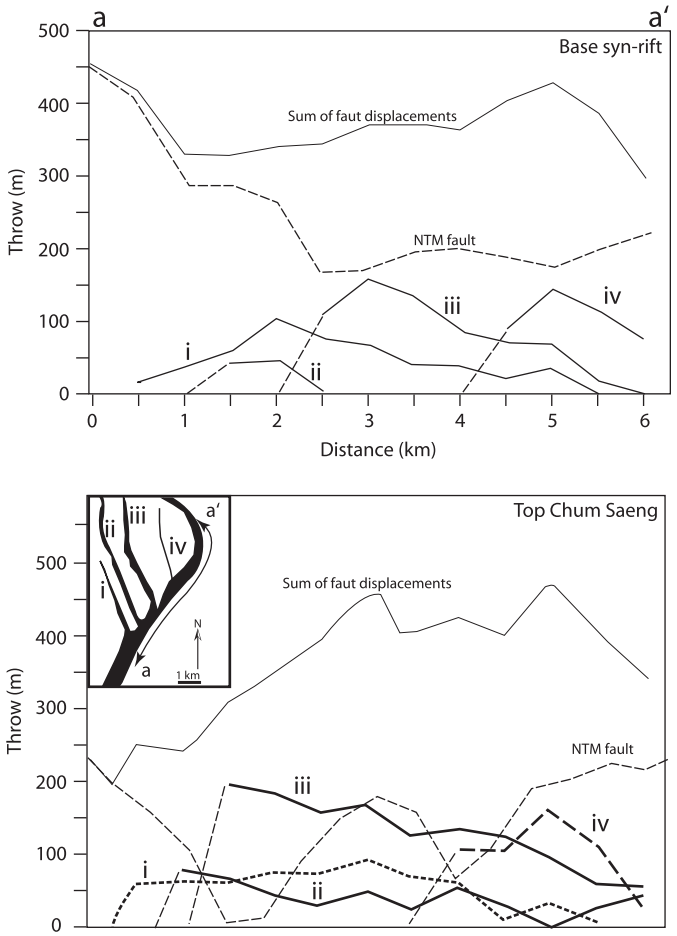

Fig. 13. Displacement vs. distance plots for the NTM-1 fault and associated N–S splays, showing the how the total displacement on the fault systems suggests displacement transfer between the faults for offsets at the base syn-rift and top Chum Saeng horizons.

the throw of the NE–SW trend is added to the throw along the N–S faults then the total displacement pattern at the base syn-rift and top Chum Saeng horizons is quite smoothly changing, and suggests transfer of displacement between the different faults. Although the faults are operating together, the key fault of interest economically is the NTM-1 fault because it is an oblique trend that is needed to provide the southern component of closure to hydrocarbon traps. A series of 3D seismic lines crossing the fault zone are shown in Fig. 14.

The finite throw pattern on fault NTM-1 shows a fault of apparently two distinct halves. The southwestern NE–SW striking segment which shows throw decreasing upwards from the base syn-rift, and the northeastern, N–S striking fault segment, where the maximum displacement lies within the syn-rift section and dies out towards the base syn-rift (Fig. 15a). Where fault displacement decreases downwards through sedimentary units there is the implication that the fault nucleated within the sedimentary section and is relatively young. The upper fault tip (zero displacement) lies buried in the subsurface along the N–S striking fault segment whilst the fault cuts to the surface along the NE–SW striking segment. At location 'a' (Fig. 15) there is a local displacement maxima within the sedimentary section, which could be interpreted as a fault segment nucleated within the sedimentary section linking with a fault that propagated up from basement.

By analysing the displacement patterns of individual horizons more details can be obtained about how the fault propagated and joined, which can test the inferences from the finite displacement patterns. Fig. 15b shows the variation in displacement vs. strike distance for key horizons. Fig. 15c represents the displacement at one interval subtracted from the next highest interval (e.g. Main Seal–S4, S4–S3 etc.). If the deeper value is less than the higher value a negative number arises, this suggests no growth i.e. no displacement occurred during that interval, and so a value of zero is given to any negative number. The method approximates how much displacement occurred for a particular time interval and it referred to here as interval displacement. The data suggest the following. Fig. 15 shows there are three places along the NTM-1 fault where displacement decreases upwards, with greatest throw occurring at the base of the syn-rift section: the southern area of the fault, and around locations 1 and 2. This pattern suggests early segments of the NTM-1 fault were active during Lan Krabu Formation times. NE of location 3 and south of location 1 the Chum Saeng Formation shows greater displacement than the base syn-rift. This pattern suggests these locations were gaps between the NTM-1 fault during Lan Krabu Formation times, with the southern segment a, linked with faults i, ii, and iii, and a separate northern segment b (Figs. 3 and 13). The absence of displacement at the Chum Saeng level, but presence of the fault both above and below the unit can be seen in Fig. 14c. It was only after Chum Saeng Formation times that displacement on the fault caused linkage into one fault. This linkage occurred during the late rift stage. Fig. 15 shows that for the NTM-1 fault separate fault segments

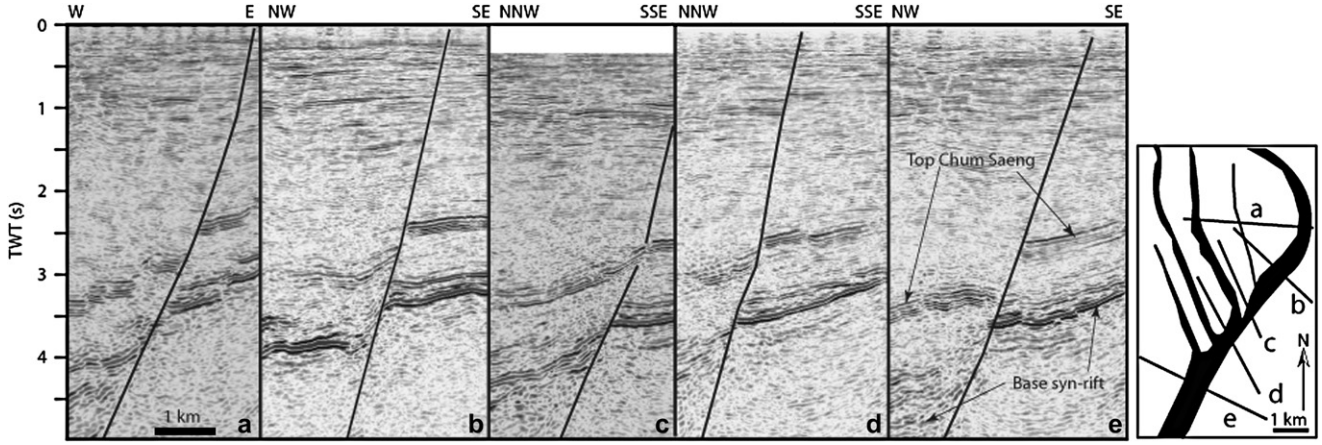

Fig. 14. Series of 3D seismic lines crossing the NTM-1 fault illustrating the general fault geometry and how offset of horizons changes along strike. Seismic line c corresponds with location 2 in Fig. 15.

have been joined late in their history (the last five million years) in some areas by the late fault system. This poses a problem for trap timing with respect to hydrocarbon migration, and may also lead to a problem regarding low displacement in areas of critical closure. There are two points along the fault (Fig. 15 linkage points at locations 2 and 3) where the fault system has joined. Hence although the fault can be mapped as a lateral closure, that lateral closure at the linkage points occurred late in the history of the fault zone. This late linkage can explain why the northeastern blocks in the NTM area failed to trap hydrocarbons, whilst the southwestern blocks are productive (Fig. 3).

During main rift times the NE–SW trend shows relatively high displacements but apparently isolated segments were not fully linked. During the late rift stage the NE–SW trend became fully linked by low displacement faults. The fault tip propagated to surface along NE–SW trend. However along the N–S trends (i, ii, iii and iv, Fig. 3) the fault tips lie buried deeper in the subsurface, indicating reactivation was less along the N–S trends, which is an oblique trend with respect to the late stress field.

6. PTO Fault history

Variations in throw for mapped horizons (base syn-rift; Chum Saeng Formation, S4, S3, S2 and S1; the S horizons lie within the Pratu Tao Formation) are shown in Fig. 16. Fig. 16a is the depth to the fault tip, which shows in general the fault tip lying deeper as the fault displacement dies out to the north. At location b there is a marked drop in displacement and increasing depth to the fault tip. Fig. 16b shows the throw values measured for each horizon, whilst Fig. 16c is interval displacement. The overall trend shows decreasing displacement from south to north. The southern region shows no offset at the base syn-rift level. There is a jump in the displacement at the base syn-rift horizon north of linkage point 1, as the fault is joined by a basement-involved fault. The data suggest the following:

The PTO fault does not show any persistent, clearly defined segments; low displacement areas on the faults marked a, b and 1 and 2 only are apparent for one or a few units. The location of areas with high displacement along the fault zone has changed with time. For the base syn-rift to Chum Saeng interval only the northern part of fault zone was active. From Chum Saeng-mid Pratu Tao Formation times the main displacement was focused on the middle part of the fault zone (Fig. 16c). During the remainder of the Pratu Tao Formation the entire length of the fault zone studied was activated, although the location of the highest displacement areas did vary with time, and a persistent area of low displacement (location 2, Fig. 16) did develop in the northern part of the fault. Post-Pratu Tao Formation the fault displacement pattern changed considerably. The strong post S1 growth is indicated by wedge-shaped expansion of reflections into the fault, that is particularly strong between depths of 1250 and 500 m on the 3D seismic data (i.e. Yom-Ping Formations). The fault zone became longer than it was in the underlying intervals extending 3 km south of the portion of the fault shown in Fig. 16, following the trend of southerly increasing displacement shown in Fig. 16c.

7. Western Boundary Fault

The Western Boundary Fault is by far the largest single fault in the northern half of the Phitsanulok basin, and has accommodated most of the strain in the basin. In terms of seismic moment, this fault and the Uttaridit Fault (Fig. 2) are likely to have been the only significant faults in the northern half of the basin. The Western Boundary fault bounds a half graben basin, but is unusual in that it is very low angle (dips between 23° and 30°) for much of its length. The fault is 60 km long and in the north the fault curves sharply to the ENE, where it follows the trend of the Palaeozoic Nan-Uttraditt Suture (Fig. 2). The main part of the fault trend is low-angled, but as the fault dies out to the south, it steepens up to over 45°. Fault heave measured from seven 2D seismic

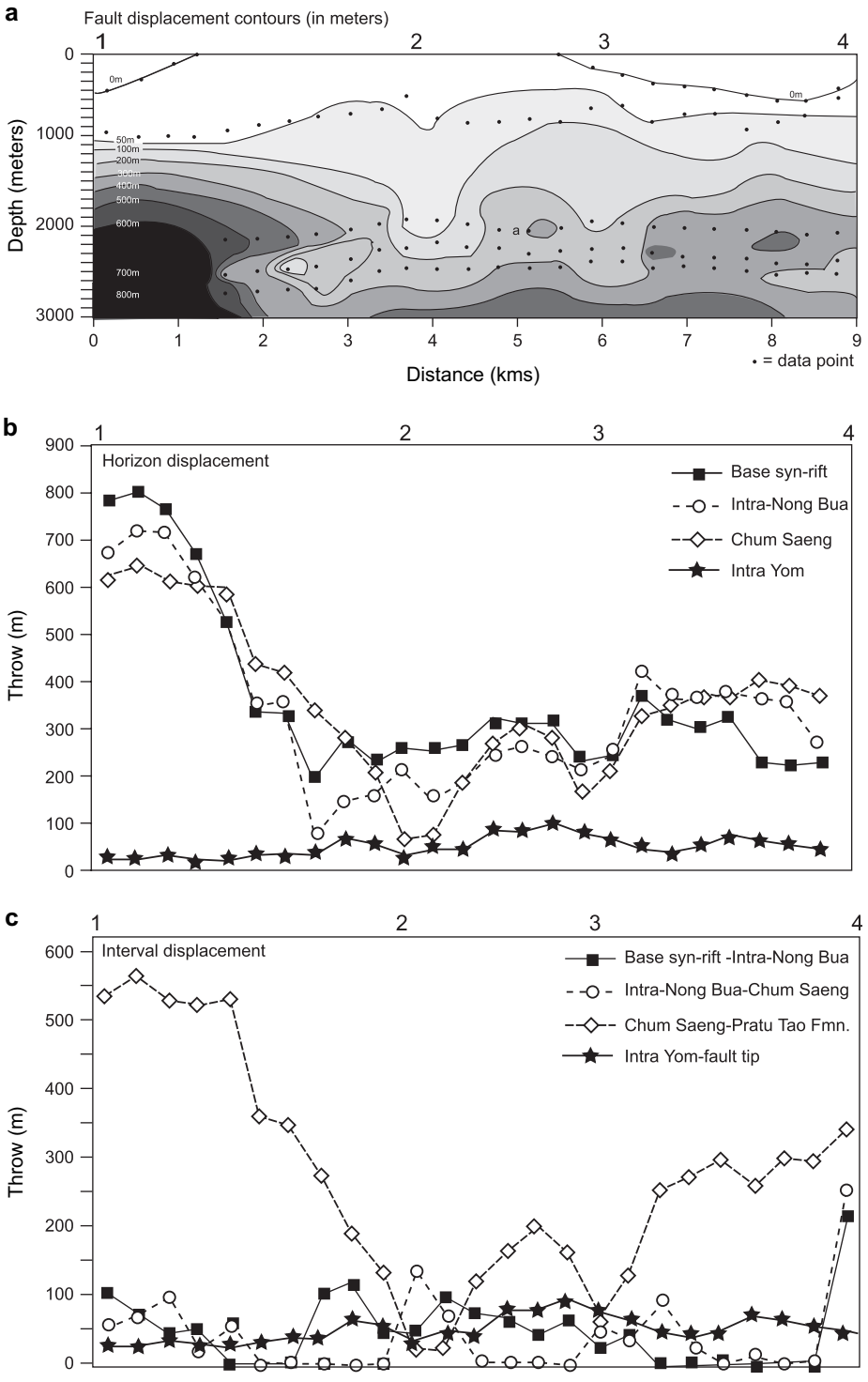

Fig. 15. Displacement (throw) characteristics of the NTM-1 Fault. (a) Displacement contours. (b) Displacement values for individual horizons along the strike of the fault. (c) Interval displacement. Interval displacement uses the displacement values in (b) and is the product of subtracting values of the shallower horizon from the deeper horizon. If the fault displays typical growth fault characteristics then the result will be a positive number and suggests fault motion during the time of the interval, or the area lies within a part of the fault that is dying out upwards. Any negative value is displayed as zero on the figure, and suggests that that particular area of the fault only experienced displacement before or after deposition of the interval. See Fig. 3a for location.

lines shows maximum displacement in the centre of the fault dying out to the north and south (Fig. 17). Fault throw does not clearly show the northwards decrease in displacement towards the fault tips because at the abrupt curve in fault trend the displacement of the horizons is not well defined on 2D data and strain becomes abruptly distributed onto the Uttaradit Fault zone. For individual horizon displacements the Late Oligocene shows relatively low amounts of displacement as

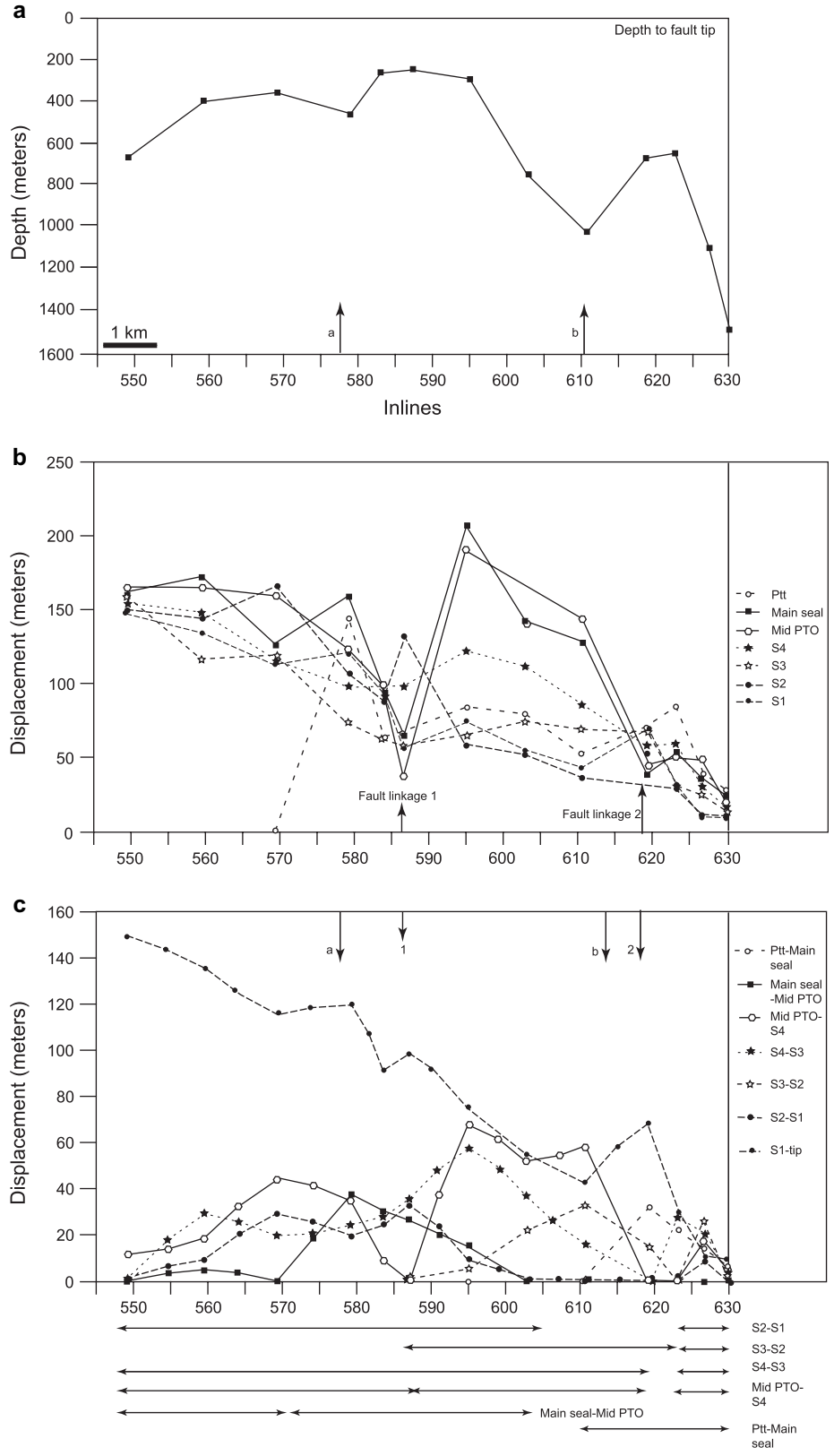

Fig. 16. Displacement characteristics and history of the PTO Fault. (a) Depth to fault tip, (b) horizon displacement, (c) interval displacement. See Fig. 3a for location.

rifting began. Average displacement rate increased in the Early Miocene, with maximum displacement in the centre of the fault. Then between about 20 Ma and 10 Ma the largest heaves were achieved, and the displacement maxima migrated north.

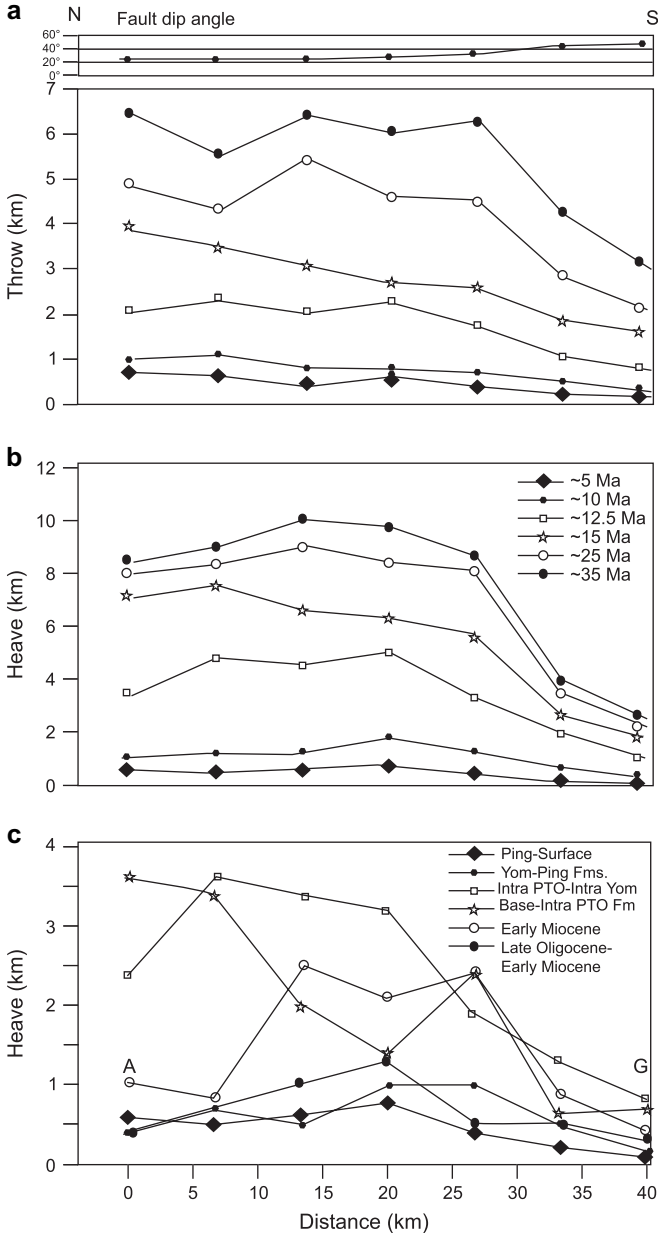

Fig. 17. Displacement characteristics of the Western Boundary Fault. (a) Horizon throw, (b) horizon heave, (c) interval heave. Displacement north of location A on the Western Boundary Fault decreases significantly in a complex zone of displacement transfer, as the oblique Uttardit Fault zone takes up much of the displacement. Note that although the interval heave shows which units show the greatest displacement, it does not show when the maximum displacement rate occurred. However in this case the highest displacement units (coinciding with the Pratu Tao Formation) also display the fastest time-averaged displacement. The approximate durations of the intervals are as follows: Ping-Surface ~5 Ma, Yom-Ping Fmns ~5 Ma, Intra PTO-Intra Yom ~2.5 Ma, Base to Intra PTO Fmn. ~2.5 Ma, Early Miocene ~8 Ma. Oligocene–Early Miocene, the age span of this unit is very poorly known, could be as much as 10 Ma. PTO, Pratu Tao Formation. Early Miocene comprises the Lan Krabu and Chum Saeng Formations.

This migration north resulted in the largest displacement occurring on the lowest-angle (23°-30°) part of the fault. This activity in turn implies the stress orientations must have been highly favourable for displacement, and/or the fault zone was very weak (either due to weak fault zone rocks or the presence of overpressured fluids) in order for high displacement to occur on a low-angle extensional fault. In the Late Miocene average displacement amount decreased significantly, particularly in terms of time–average strain rate (maximum heave displacement rate for Pratu Tao Formation is about 1.4 mm/year, whilst for the Yom-Ping Formation it is 0.4 mm/year, Fig. 4). The region of maximum displacement shifted to the south to lie near the centre of the fault in the Late Miocene–Pliocene.

8. Discussion

A number of the rift and post-rift basins in Thailand are deformed by very numerous, low displacement (tens of metres of throw) normal faults, many have a conjugate geometry. These faults are well imaged on extensive 3D seismic data sets. The Phitsanulok basin contains hundreds of such faults. Offset of horizons by the faults shows that for the vast majority of faults the greatest offsets occur between depths of about 1 and 3 km within the sedimentary section. Passing vertically downwards the faults partially or completely lose displacement towards the deepest reflection: the base of the syn-rift section. In a few areas it is possible to see that locally the main faults in the basin are completely detached from faults affecting basement and the lowest syn-rift section. The younger faults do not link with the older faults, and terminate at the top basement reflection or higher in the section. The presence of NE–SW trending faults north of the NTM-1 fault (Fig. 9) that overlie N–S trending faults at the Chum Saeng level clearly illustrate the presence of faults nucleated from within the sedimentary section, which die out downwards within the sedimentary section. These faults are only slightly listric and do not systematically join detachments in sedimentary units in the fashion of typical gravity-driven normal fault systems. They appear to be formed as a response to crustal stresses.

Variations on the basin-nucleated pattern are commonly repeated in offshore basins too, such as the Pattani and North Malay basin (Kornsawan and Morley, 2002; Morley et al., 2004). Seismic data quality is good, and there is no reason to doubt the observation. These patterns suggest that there is a strong difference between the way the pre-rift 'basement' and the sedimentary basin accommodated strain. This pattern is best seen in the smaller faults, and is not seen in the largest rift boundary faults. The intermediate size faults discussed in this paper (Figs. 11, 13–16) show a mixed history where basement-nucleated faults and basin-nucleated faults have combined with time as illustrated schematically in Fig. 18. Presumably this late stage deformation reflects relatively low differential stresses that are able to deform weaker sedimentary rocks, but not stronger pre-Cenozoic rocks. How the strain seen in the Tertiary

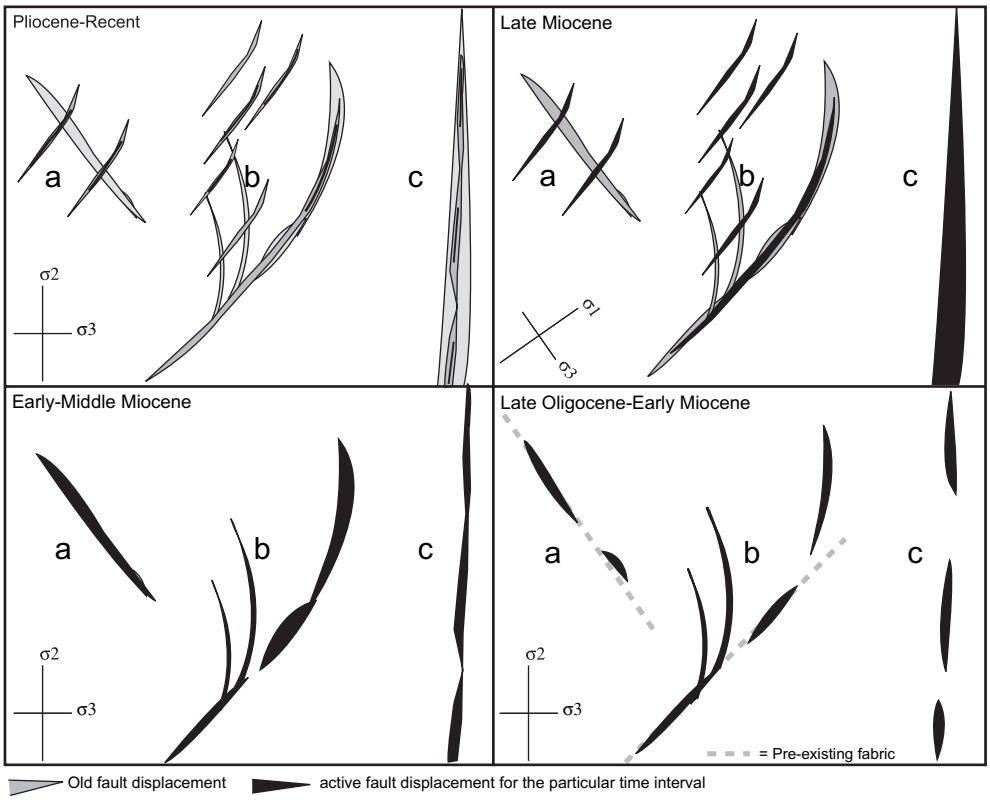

Fig. 18. Schematic illustration of the displacement evolution on fault trends of different orientation through time. Late Oligocene–Early Miocene, NW–SE and NE–SW pre-existing trends followed by short faults. Early–Middle Miocene, N–S trend is fully linked, displacement builds on NE–SW trends, but they fail to link. Late Miocene–Recent, Stress state changes to ENE–WSW to NE–SW Shmax. NW–SE trend, ignored, new NE–SW oriented faults created. NE–SW trend (b) becomes entirely linked displace small, late displacement. N–S trend, widely activated, but throw is patchy and variable. Pliocene–Recent return to N–S Shmax and extension, but displacements are very low.

basin is accommodated within the pre-Cenozoic is uncertain, possibly it occurred along larger more widely spaced faults, such as the Western Boundary, Uttaradit and NTM-1 fault zones.

It is generally thought that in a simple progressive extensional opening of a rift normal fault populations will show the effects of linkage with time. These effects will tend to reduce the number of active small faults, and increasingly concentrate deformation on larger faults (e.g. Cowie, 1998; Gupta et al., 1998; Nicol et al., 2005a,b). The larger faults commonly tend to show increasing displacements with time. However the Phitsanulok basin has shown that where extensional stresses change orientation with time, or evolve to transpressional stresses, this simple development may not occur. First instead of the evolution to larger faults with shorter faults becoming less active, in the GPTOS area the late rift stage is characterised by new sets of numerous, short strike-length, low displacement faults. Accompanying this change late-stage, long faults were created by linkage of isolated higher displacement older faults, by late, widespread but low displacement offsets. Fully linked N–S striking faults such as PTO-1 showed a return to more patchy slip distribution during the late-rift event, inferred to be due to non-optimal orientation with respect to the late stress field.

9. Conclusions

In the Northern Phitsanulok basin three main stress states have been identified associated with Late Oligocene–Recent fault development: (1) Late Oligocene–Late Miocene approximately E–W extension (N–S Shmax), ‘main rift’ stage, (2) Late Miocene–Pliocene transtension to tranpression (?) (E–W to NE–SW Shmax, inferred to be locally NE–SW for the GPTOS area), ‘late rift’ stage, and (3) Pliocene–Recent very minor faulting, E–W extension, N–S Shmax, ‘post-rift’ stage.

The largest fault in the basin, the Western Boundary Fault displays little discernible difference in the distribution of displacement on fault zone during the different stress states other than increases and decreases in displacement amount. The complexity of basin evolution is best seen in the smaller fault sets where the linkage of the fault zone has commonly been delayed until later in the basin history, or linked faults revert to slip only in discrete areas of the fault. These smaller faults exhibit a more selective reactivation history than the Western Boundary fault and consequently the displacement characteristics of the smaller fault zone are more informative about fault response to a varying stress field. It may well be that the Western Boundary fault did respond in a similar fashion to the smaller faults, but large

extensional displacement has masked or destroyed the evidence.

Activation of the NE–SW striking NTM-1 Fault during the main rift stage failed to produce a fully linked fault, despite the fault segments showing relatively large displacements. Hence it is inferred that relatively strong segments were effective in halting fault propagation when the fault lay oblique to the regional extension direction. When stresses reoriented during the late rift stage, the NE–SW striking faults became more favourably oriented for reactivation, and despite displaying overall lower interval displacement than during the main rift stage, finally became linked in the Late Miocene.

Standard fault seal analysis considers: (1) juxtaposition seal, (2) membrane seal, and (3) potential for fractures to open due to modern stress state. Generally trap timing with respect to hydrocarbon migration is not considered as an issue, except in black and white terms: either the fault was present before or after migration occurred. However, due to partial linkage of the fault zone the NTM-1 fault had 'holes' at the time of migration. Consequently certain trapping configurations may be bypassed, whilst others have an effective fault seal and are able to trap hydrocarbons. This evolution can explain why the southwestern part of the NTM-1 fault acted as a seal to hydrocarbon bearing reservoirs, whilst the area between points 2 and 3 (Fig. 13), which are late linkage points, failed to seal hydrocarbons.

The N–S striking PTO-1 Fault shows early isolated fault segments. During Pratu Tao Formation times (peak displacement on the Western Boundary Fault) a unifying displacement gradient, with displacement decreasing from south to north, was imposed on the more disparate earlier displacements. The latest, minor displacements indicated by variations in the depth to the fault tip point to a reversion to more patchy distribution of displacement late in the fault history, perhaps due to non-optimal orientation of the fault to the regional stress field, when compared with the NTM-1 Fault. Slipped patches that define segmentation within a fault are not necessarily persistent features throughout the life of the fault. For fault PTO-1 the present day irregularities in the upper fault tip geometry (Fig. 14) does not match the location of early displacement lows.

During the Late Miocene a distinctly different type of fault population from the main rift set evolved, characterised by numerous, small displacement (tens of metres) faults. Where these late rift faults formed independently of the many main rift faults they tend to strike NE–SW. Where late rift faults reactivated older fault trends strike directions between 350° to 50° are favoured. One key feature of the late faults is their nucleation within the sedimentary section of the basin, not the pre-rift 'basement'. These basin nucleated faults are a common feature of the late stage deformation in the rift basins of Thailand.

Acknowledgements

We would like to thank PTT Exploration and Production for permission to publish the data, and Conrad Childs and an anonymous reviewer for constructive comments that considerably helped improve the manuscript.

References

Bal, A.A., Burgisser, H.M., Herber, M.A., Rigby, S.M., Thumpraesertwong, S., Winkler, F.J., 1992. The Cenozoic Phitsanulok basin, Thailand. National Conference on the Geological Resources of Thailand: Potential for Future Development. Department of Mineral Resources, Bangkok, Thailand. pp. 247–258.

Barnett, J.A.M., Mortimer, J., Rippon, J.H., Walsh, J.J., Watterson, J., 1987. Displacement geometry in the volume containing a single normal fault. AAPG. Bulletin 71, 925–937.

Cartwright, J.A., Trudgill, B.D., Mansfield, C.S., 1995. Fault growth by segment linkage: An explanation for scatter in maximum displacement and trace length data from the Canyonlands Grabens of SE Utah. Journal of Structural Geology 17, 1319–1326.

Cowie, P.A., 1998. A healing-reloading feedback control on the growth rate of seismogenic faults. Journal of Structural Geology 20, 1075–1087.

Cowie, P.A., Schloz, C.H., 1992. Displacement-length scaling relationship for faults: data synthesis and discussion. Journal of Structural Geology 14, 1149–1156.

Davison, I., 1994. Linked fault systems; extensional, strike-slip and contractional. In: Hancock, P.L. (Ed.), Continental Deformation. Pergamon Press, Oxford, pp. 121–142.

De Paola, N., Holdsworth, R.E., McCaffrey, K.J.W., Barchi, M.R., 2005. Partitioned transtension: an alternative to basin inversion models. Journal of Structural Geology 27, 607–625.

Flint, S., Stewart, D.J., Hyde, T., Gevers, C.A., Dubrule, O.R.F., Van Riessen, E.D., 1988. Aspects of reservoir geology and production behaviour of Sirikit Oil Field, Thailand: an integrated study using well and 3-D seismic data. American Association of Petroleum Geology Bulletin 72, 1254–1268.

Gupta, S., Cowie, P.A., Dawers, N.H., Underhill, J.R., 1998. A mechanism to explain rift-basin subsidence and stratigraphic patterns through fault-array evolution. Geology 26, 595–598.

Huggins, P., Watterson, J., Walsh, J.J., Childs, C., 1995. Relay zone geometry and transfer between normal faults recorded in coal-mine planes. Journal of Structural Geology 17, 1741–1755.

Knox, G.J., Wakefield, L.L. 1983. An introduction to the Geology of the Phitsanulok Basin. Conference on Geology and Mineral Resources of Thailand, Bangkok, 19-28 November, p. 9.

Kornsawan, A., Morley, C.K., 2002. The origin and evolution of complex transfer zones (graben shifts) in conjugate fault systems around the Funan Field, Pattani basin, Gulf of Thailand. Journal of Structural Geology 24, 435–449.

Morley, C.K., 1999a. Patterns of displacement along large normal faults: Implications for basin evolution and fault propagation, based on examples from East Africa. American Association of Petroleum Geology Bulletin 83, 613–634.

Morley, C.K., 1999b. Tectonic inversion in East African rifts. In: Morley, C.K. (Ed.), Geoscience of Rift Systems—Evolution of East Africa. American Association of Petroleum Geology Studies in Geology, 44, pp. 193–210.

Morley, C.K., 2007. Variations in Late Cenozoic-Recent strike-slip and oblique-extensional geometries within Indochina: the influence of pre-existing fabrics. Journal of Structural Geology 29, 36–58.

Morley, C.K., Wonganan, N., 2000. Normal fault displacement characteristics, with particular reference to synthetic transfer zones, Mae Moh Mine, Northern Thailand. Basin Research 12, 1–22.

Morley, C.K., Sangkumarn, N., Hoon, T.B., Chonglakmani, C., Lambiase, J., 2000. Structural evolution of the Li Basin northern Thailand. Journal of the Geological Society of London 157, 483–492.

Morley, C.K., Woganan, N., Sankumarn, N., Hoon, T.B., Alief, A., Simmons, M., 2001. Late Oligocene–Recent stress evolution in rift basins of Northern and Central Thailand: Implications for escape tectonics. Tectonophysics 334, 115–150.

Morley, C.K., Wonganan, N., Kornasawan, A., Phoosongsee, W., Haranya, C., Pongwapee, S., 2004. Activation of rift oblique and rift parallel pre-existing fabrics during extension and their effect on deformation style:

Examples from the rifts of Thailand. Journal of Structural Geology 26, 1803–1829.

Nicol, A., Walsh, J., Berryman, K., Nodder, S., 2005a. Growth of a normal fault by the accumulation of slip over millions of years. Journal of Structural Geology 27, 327–342.

Nicol, A., Walsh, J.J., Manzocchi, T., Morewood, N., 2005b. Displacement rates and average earthquake recurrence intervals on normal faults. Journal of Structural Geology 27, 541–551.

Peacock, D.C.P., Sanderson, D.J., 1991. Displacements, segment linkage and relay ramps in normal fault zones. Journal of Structural Geology 13, 721–733.

Schlische, R.W., 1991. Half-graben basin filling models: new constraints on continental extensional basin development. Basin Research 3, 123–141.

Schlische, R.W., Anders, M.N., 1996. Stratigraphic effects and tectonic implications of the growth of normal faults and extensional basins. Geological Society of America Special Paper 303, 183–203.

Talbot, M.R., Morley, C.K., Le Herrise, A., Tiercelin, J.-J., Gall, Le, Potdevin, B., Maende, J.-L., Vetel, W., 2005. Hydrocarbon potential in the Meso-Cenozoic Turkana Depression, Northern Kenya, II-Source rocks: depositional environments, diagenetic characteristics and regional structure. Marine and Petroleum Geology 21, 63–78.

Walsh, J.J., Watterson, J., 1987. Distribution of cumulative displacement and of seismic slip on a single normal fault surface. Journal of Structural Geology 9, 1039–1046.

Walsh, J.J., Watterson, J., 1988. Analysis of the relationship between displacements and dimensions of faults. Journal of Structural Geology 10, 239–247.

Walsh, J.J., Watterson, J., 1992. Populations of faults and fault displacements and their effects on estimates of fault-related regional extension. Journal of Structural Geology 14, 701–712.

Young, M.J., Gawthorpe, R.L., Hardy, S., 2001. Growth and linkage of segmented normal faults zone: the late Jurassic Murchison–Statfjord North Fault, northern North Sea. Journal of Structural Geology 23, 1933–1952.